Observation of temporary-negative-ion states in condensed methanol via vibrational excitation induced by slow electron scattering

A. T. Wen, M. Michaud, and L. Sanche*
Département de Médecine Nucléaire et Radiobiologie, Faculté de Médecine, Université de Sherbrooke, Sherbrooke, Québec, Canada J1H 5N4
(Received 3 April 1996)

We report the measurements of electron-impact vibrational excitation of amorphous methanol condensed on a polycrystalline Pt substrate over incident energies of 1–20 eV at a large off-specular angle. The spectra obtained show that vibrations within solid methanol in its ground state are rather sensitive to the variation of impact energy and there is tangible evidence of the formation of at least three compound temporary-negative-ion (TNI) states. The low-energy feature lying between 3 and 6 eV is assigned tentatively to a $^2A'$ valence-shape resonance with a $^2[N,(8a'\sigma^*)^1]$ configuration, whose parent state is the ground state $^1A'$ of the molecule. The origin of the second broad structure centered around 7.0 eV in the excitation functions may be threefold: a Feshbach-type resonance $^2A''$ of the electronic configuration $^2[(2a'')^1,(3sa')^2]$ (about 7 eV); a nearby shape resonance $^2A'$ of $^2[(N,(9a'\sigma^*)^1]$ (about 8 eV); and probably also a minor contribution from another $^2[(7a')^1,(3sa')^2]$ Feshbach resonance $^2A'$ (about 9 eV). The third broad bandlike resonant feature, extending from 11 up to 17 eV, may consist of overlapping TNI states, dominated by the $^2[(6a')^1,(3sa')^2]$ Feshbach resonance $^2A'$. Plausible decay channels from their configurations are discussed. [S1050-2947(96)09011-7]

PACS number(s): 79.20.Kz, 34.80.Gs, 79.60.Dp, 77.55.+f

I. INTRODUCTION

The scattering of low-energy (0–20 eV) electrons from molecules adsorbed on surfaces often leads to considerable enhancement of vibrational excitation of intramolecular modes within the adsorbate, owing to the formation of temporary negative ion (TNI) states, in which the incident electron is temporarily captured in the vicinity of the adsorbate and simultaneously triggers a perturbation of equilibrium internuclear distances [1]. The phenomenon, usually referred to as resonance electron scattering, has been observed, using high-resolution electron-energy-loss (HREEL) spectroscopy, in both strongly (chemisorption) and weakly (physisorption) bound absorbate-surface systems. While the former can be depicted by the case studies of benzene chemisorbed on Pd(100) (Ref. [2]) and CO on Ni(110) (Ref. [3]), the latter may be demonstrated by examples of N_2 and O_2 adsorbed on Ag films [4]. In addition, resonance scattering also finds its way into molecular solids condensed on a metal surface. This can be seen in some of the work of this laboratory, such as solid O_2 deposited on polycrystalline niobium [5], and amorphous N_2, CO, and H_2O deposited on polycrystalline platinum [6,7].

We report in this paper experimental work on resonant vibrational excitation of an organic solid, that is, methanol, the simplest of alcoholic species. Methanol may be regarded as a methylated derivative of H-OH and hence its low-energy electron-scattering spectroscopy may be expected to resemble that of water, which is of particular relevance in improving our understanding of the effects of ionizing radiation on the human body and other biological media [8]. Very often, the substitution of an electron-repelling group CH_3 for H increases the energy of the TNI state [9], thus destabilizing the resonance state and consequently shortening its lifetime. This should be reflected in our present measurements of TNI states. Although methanol is widely employed in synthetic chemistry and biochemistry as a solvent and/or starting material, our knowledge of resonance electron scattering from it has, however, been limited to a single early effort made by Mathur and Hasted [10]. They observed with an electron-transmission spectrometer a broad hollow feature between 6 and 10 eV in the total scattering cross section function of vapor-phase CH_3OH but gave no specific assignment. In the more recent dissociative electron attachment (DEA) studies of Kühn, Fenzlaff, and Illenberg [11], Curtis and Walker [12], and Parenteau, Jay-Gerin, and Sanche [13], resonances were identified by observing the dissociated anion fragments in the stable anion yield. Their findings were necessarily limited to *dissociative* TNI states that have lifetimes of the same order of or longer than a vibrational period. Although it has been known that a much more complete picture of the TNI manifold of methanol may be obtained from incident-energy dependences of vibrational excitation (i.e., excitation functions), the direct observation of TNI resonant states in methanol through vibrational excitation induced by low-energy electrons is still not available, to the best of our knowledge, even in the vapor phase.

In the present study, which is an extension of the electron-energy-loss work of Michaud, Fraser, and Sanche [14] on methanol, we have measured with HREEL spectroscopy vibrational excitation and its corresponding excitation functions for solid films of methanol in the energy range 1–20 eV at a large off-specular angle. Because of the use of a relatively thick film (30 layers) in our experiment, to ensure that the results are independent of the film thickness and the reflectivity of the substrate, multiple elastic and inelastic scat-

*Author to whom correspondence should be addressed.

tering events within the film become inevitable [15,16]. This may introduce some common extra features into a scattering spectrum [6,7], thus making the elastic and vibrational excitation functions look similar at first glance. The phenomenological origin of such an apparent similarity is considered to be twofold: (a) the existence of a common multiple inelastic-scattering background, and (b) the modulation by the elastic reflectivity (i.e., multiple elastic scattering before and after an inelastic-scattering event). In our study of the resonance scattering contribution to the vibrational-excitation functions of methanol, the former effect is simply removed by subtracting the closest background, whereas the assessment of the latter relies essentially upon a rigorous comparison (e.g., accurate energy positions of the maxima) between the elastic and the various vibrational-excitation functions. In this work, we show that by measuring and analyzing carefully incident-energy dependences for some physically meaningful ''background'' losses, the scattering intensities arising from the multiple-scattering effect [16] can be diminished sufficiently, and obscured genuine spectral features can therefore be better observed. We present here the resulting data showing the pronounced effect of the incident electron energy on the intensity and line shape of some vibrational energy losses, and report our observation of electron-scattering resonances in solid methanol through both energy-loss spectra and vibrational-excitation functions.

II. EXPERIMENTAL DETAILS

The apparatus used in the present work has already been described in detail by Sanche and Michaud [6], and therefore only a brief description of the salient features is given here. The electron spectrometer is housed in a cryopumped UHV system reaching a typical base pressure of 4×10^{-11} torr. An energetically well defined electron beam (0.2∼0.4 nA) emerging from a single hemispherical monochromator impinges upon a polycrystalline Pt ribbon cleaned by resistive heating within the UHV chamber. The ribbon is pressed tightly against the cold tip of a closed-cycle cryostat to reach the working temperature of 15 K. Electrons reflected from the Pt surface are focused into a second similar hemispherical energy analyzer fixed at 45° with respect to the surface normal. In the electron optics, two double-zoom lens systems, which are placed at the exit of the monochromator and the entrance of the analyzer allow us to measure with ease an excitation function over a wide range of incident energy (e.g., 1–20 eV). The monochromator can be rotated over an angular range of $14°\leqslant\theta_0\leqslant70°$ relative to the normal, allowing differential cross sections to be measured. The spectrometer was adjusted to an overall energy resolution of 9–10 meV, determined by the full width at half maximum (FWHM) of the elastically backscattered peak. The incident electron energy (E_0) was calibrated against the vacuum level, within ±0.05 eV, by measuring the onset of the electron current transmitted through the condensed films.

Reagent-grade anhydrous methanol (99.95%) purchased from Aldrich Chemical Ltd. was degassed by several freeze-pump-thaw cycles before being leaked into the UHV system through a capillary tube whose end is located just in front of the Pt ribbon [6]. The purity of the sample was further examined *in situ* by mass spectroscopy.

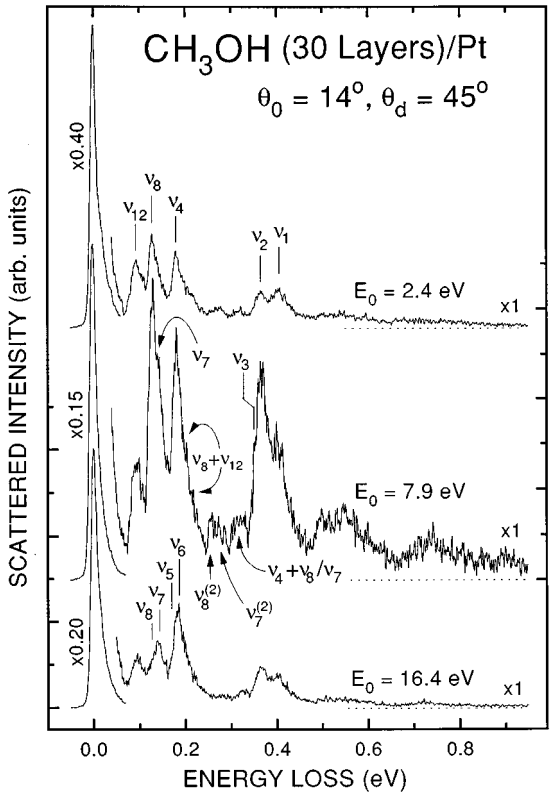

FIG. 1. Vibrational electron-energy-loss spectra obtained for a 30-layer solid methanol film deposited on a polycrystalline platinum foil held at 15 K. The incident electron-beam energies E_0 are 2.4, 7.9, and 16.4 eV. The incoming beam is oriented at 14° relative to the surface normal and the scattered electrons are detected at 45° with respect to the normal. Except for their elastic peak, all spectra are plotted with the same gain to best illustrate the effect of resonance electron scattering. A strong resonant enhancement of various vibrational modes is manifested in the 7.9-eV spectrum; the dependence of different vibrational frequencies on impact energy is clearly visible.

III. RESULTS AND DISCUSSION

A. Electron-energy-loss spectra

Three typical representative HREEL spectra of 30-layer CH_3OH films are given in Fig. 1, where a strong incident-energy dependence of energy-loss intensities is evident. Though not presented here, the angular dependence of the intensities was also examined at different film thicknesses. The results showed essentially that the intensity contribution from the long-range dipole interaction (i.e., the dipole lobe) observed near the specular beam direction (45°) at monolayer coverage diminished considerably at higher coverages and was suppressed effectively above 8∼10 layers in our solid CH_3OH/polycrystalline Pt system [17].

The vibrational modes and frequencies derived for solid methanol from the early infrared work of Falk and Walley [18] are summarized in Table I. Most of these modes are clearly present in Fig. 1. Although with the current instrumental resolution a decisive assignment for every mode is not always realistic and reliable, the proposed assignments involving the fundamentals are also tabulated in Table I. A full account of the methanol vibrational-energy losses asso-

TABLE I. Comparison of the vibrations (meV[a]) in the IR spectra of solid methanol with the observed vibrational energy losses (meV) in the HREEL spectrum of methanol condensed on a 15 K polycrystalline Pt foil.

Symmetry species	No.	CH_3OH amorphous solid, 93 K (Ref. [18])	CH_3OH on polycrystal Pt foil, 15 K (this work)	CH_3OH crystal 93 K (Ref. [18])	Approximate type of mode
a'	ν_1 (IR,R)[b]	401.1 (vs)[c]	407±1 (s)	426.9 (sh)	ν(OH) stretch
			396±2 (s)	407.2 (vs)	
				395.2 (s)	
a'	ν_2 (IR,R)	369.7 (sh)	368±1 (vs)	369.7 (m)	$\nu(CH_3)$ asymmetric stretch
				366.4 (s)	
a''	ν_9 (IR,R)	365.9 (vs)	(360±2)[d]	361.1 (sh)	
a'	ν_3 (IR,R)	350.7 (s)	351±2 (sh)	350.8 (s)	$\nu(CH_3)$ symmetric stretch
a'	ν_4 (IR,R)	180.0 (m)	180±1 (vs)	180.8 (sh)	$\delta(CH_3)$ asymmetric bend
a''	ν_{10} (IR,R)			179.2 (m)	
a'	ν_5 (IR)	175.4 (sh)	(175±2)	176.8 (sh)	$\delta(CH_3)$ symmetric bend
a'	ν_6 (IR)	179.8 (m)	(187±2)	187.7 (m)	δ(OH) in-plane bend
				182.3 (m)	
a'	ν_7 (IR,R)	139.4 (w)	140±1 (m)	144.1 (vw)	$\rho(CH_3)$ rock
				141.6 (w)	
a''	ν_{11} (R)	155.7 (w)	155±2 (w)	155.7 (w)	
a'	ν_8 (IR,R)	128.0 (vs)	128±1 (vs)	129.7 (w)	ν(CO) stretch
				127.6 (vs)	
a''	ν_{12} (IR)	90.5 (s)	97±2 (m)	98.0 (s)	γ(OH) out-of-plane bend
			86±2 (sh)	84.9 (m)	

[a]The data in cm^{-1} have been converted to meV by the convertion factor of 8.065 cm^{-1} meV^{-1}.
[b]IR: Infrared active; R: Raman active, derived from liquid methanol.
[c](vs) very strong; (s) strong; (m) medium; (w) weak; (vw) very weak; (sh) shoulder.
[d]The figure in parentheses is not fully resolved in the HREEL spectra and mainly inferred from shoulders and/or overlapping peaks.

ciated with not merely the fundamental modes but also their combinations, overtones, and double losses will be presented in a forthcoming publication [17]. Since the emphasis of the present contribution is on resonance electron scattering, as stated in the introduction, only a few points concerning the energy-loss spectra in Fig. 1, which will be relevant to our observation of the TNI states, are discussed here as follows.

Lattice phonon modes, both translational and librational, are seemingly missing here in the HREEL spectra of solid methanol. This is in sharp contrast to what has been seen in the case of amorphous ice [7]. According to the infrared data of methanol [18], the amorphous film gives rise to only one single weak intermolecular vibrational band near 320 cm^{-1}, which would yield an energy-loss feature at approximately 40 meV. Given the fact that we have essentially the same instrumental resolution in the two studies of water and methanol, we should be able to observe this lattice mode in our HREEL spectra, as seen in amorphous ice. Perhaps the faint indication of a shoulder near 40 meV in the 2.4-eV spectrum may be associated with this optical-phonon feature, since the cross section for dipole scattering favors low impact energies. The apparent absence of it in the spectra of higher incident energies may plausibly reflect that it is relatively too weak in intensity to be detected and/or to be resolved from the elastic peak. Thus, one may expect that the multiple losses of this phonon mode would only make a rather limited contribution to the energy-loss background or to the excitation-function intensity in our spectra.

It is of particular interest to note the remarkable increase in intensity induced by the incident energy of 7.9 eV in Fig. 1, through which not only double-loss and/or combination transitions can be determined readily, but overtone excitation may also be ascertained. However, it should be pointed out that such an increase is not uniform throughout the energy-loss spectrum and a variation of the relative intensity change may be found among the different vibrational modes. For instance, while some of the spectral features in the 7.9-eV spectrum are at least three times as intense as their counterparts in the other two spectra, others are merely twice or less. The latter is evidenced by the intensities of the elastic peaks and the ν_{12} energy losses shown in the 7.9- and 16.4-eV spectra. It is worth noting at this point that within the Born-approximation framework, theoretical calculations of vibrational excitation for water [19], the parent molecule of methanol, indicate that the cross sections of different vibrational modes are reduced only slightly as the incident energy increases from 8 to 16 eV. In fact, this is almost always the case for direct excitation, because its cross section favors low-energy electrons and varies noticeably only in a very low energy bracket (<3 eV) [19]. As such, one would then expect the cross-section increase to be rather marginal also for methanol on going from 16.4 to 7.9 eV. But this would, in turn, contradict what we have seen in Fig. 1. It is thus clear that an interpretation invoking only a simple direct-

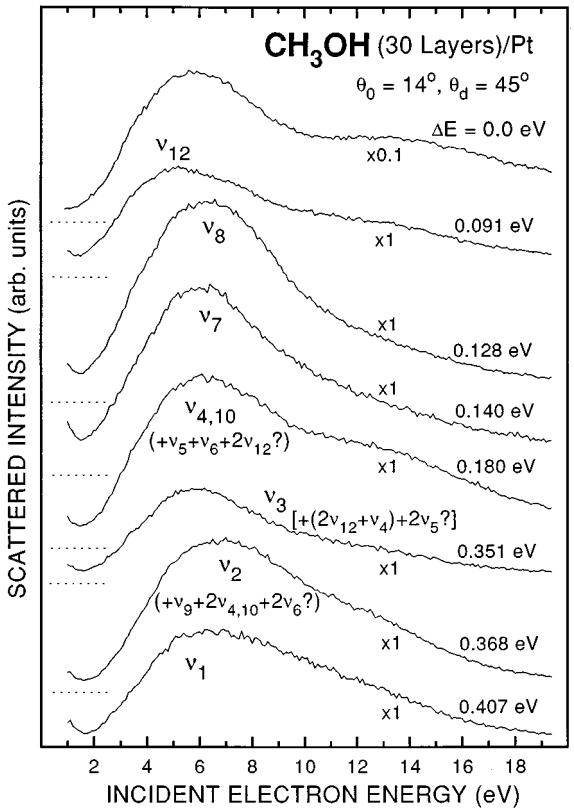

FIG. 2. Excitation functions obtained at eight selected vibrational-energy losses for a 30-layer solid methanol film. The corresponding fundamental vibrational modes of methanol are indicated for each curve and the modes that may contribute also to a specific excitation function are suggested in parentheses. The excitation functions for the fundamental frequencies are presented with the same gain in order to depict the variation in the scattering probabilities of exciting different vibrational modes in methanol.

excitation mechanism cannot be sustained.

For adsorbed molecules, there are three major different electron-molecule scattering mechanisms that have been identified so far, viz., dipole, impact, and resonance scattering [1,20]. Though favored under the present experimental conditions of incident electron energy and scattering geometry, impact scattering is unable to explain the exceptional enhancement in intensity in the 7.9-eV spectrum. Such an enhancement must then be attributed to resonance electron scattering, whose signature is generally an enhanced intensity of vibrational modes over a relatively narrow impact-energy range. Although the spectra in Fig. 1 have already provided tangible evidence of the occurrence of resonant vibrational excitation in solid methanol, resonance scattering may still be best observed through the structure that it creates in excitation functions of certain vibrational-excitation channels.

B. Vibrational-excitation functions

We have measured excitation functions for the elastic peak and major vibrational-energy losses in solid methanol and they, except for the elastic, are plotted with the same gain in Fig. 2 to best illustrate the variation in the scattering probability from exciting the different vibrational modes of methanol. It should be pointed out that the excitation functions recorded at energy losses of 180 and 368 meV for the fundamental frequencies of $\nu_{4,10}$ and ν_2 may contain contributions from the nearby fundamental modes, double losses, and/or combinations of the low-frequency modes, as suggested in Fig. 2, since they are energetically too close to each other.

It is at first sight peculiar somehow that all of these excitation functions have a roughly similar overall shape: a broad humplike feature around 6 eV followed by a tail extending over the entire high-impact-energy regime. Such collective behavior is expected when the scattered intensities corresponding to the energy-loss features include those arising from multiple-scattering processes, both elastic and inelastic, as a result of using relatively thick molecular films. In the measurement of slow electron scattering by a disordered film, the problem associated with the backscattered electron intensity can be addressed, when the angular distribution is not required, simply by solving the Boltzmann transport equation for a plane-parallel system in the ''two-stream'' approximation [15]. According to this model, for sufficiently thick films one has to deal with (a) the presence of a multiple-scattering background, upon which the single-loss features are superimposed, and (b) the occurrence of multiple elastic scattering before and after an inelastic-scattering event, which may result in an energy modulation of the single-loss features. While the former effect can be separated from the real signals through a background subtraction with a well selected background measurement, the latter, closely related to the elastic reflectivity of the film, cannot be removed, in general, by normalizing simply with the elastic intensity, since it depends also upon the degree of angular anisotropy of the inelastic event. For example, the two-stream model shows that when elastic-reflectivity values are smaller than 50%, the intensity of a single-loss feature is practically independent of the reflectivity in the isotropic scattering process, but it becomes almost proportional to the reflectivity in the case of purely anisotropic scattering [15]. Therefore, the excitation functions in Fig. 2 should not simply be normalized to that of the elastic peak. Of particular concern are also the spurious features that might be introduced into such a normalization, as they would confuse rather than facilitate the interpretation [21].

Though similar to each other in many ways, the profiles of the excitation functions still display, even before any background removal, a noticeable difference in peak position and shape among the different modes. For instance, close inspection shows that the two excitation functions associated with the two hydroxyl (OH) modes (ν_1 and ν_{12}) have their maximum near or towards 5 eV, relatively lower than the others. In addition, the excitation function of the C=O stretching vibration ν_8, a strong infrared (dipole) -active mode, does not follow the energy-dependent behavior of the elastic peak ($v=0$) in Fig. 2. Obviously, it is quite desirable to remove the multiple-scattering background as much as possible to reveal weak electron resonant features in the excitation functions. In order to eliminate the energy-dependent background, we have, along with the fundamental vibrational-excitation functions, also measured the energy-dependent distributions of four minima located at 68, 113, 165, and 340 meV (i.e., just before the four fundamental

vibrational losses of the ν_{12}, ν_8, ν_4, and ν_2 modes in Fig. 1, respectively). By subtracting the four background energy-dependent curves given in Fig. 3(a) from the corresponding excitation functions of the above-mentioned four fundamentals, we obtained four resulting *difference* functions presented in Fig. 3(b). It must be borne in mind, however, that these difference functions should be regarded as a useful complement and not by any means a replacement for the recorded excitation functions in Fig. 2.

Among the excitation function in Fig. 3(b), one can distinguish at least three energetically distinct features. An asymmetric plateau lying between 3 and 6 eV, which is mainly visible in the ν_{12}(OH) excitation function, a bell-shaped structure centered around 7 eV, which appears more clearly in the ν_8(CO) excitation function, and a relatively weak broad band extending from 11 up to 17 eV, which is seen more clearly in the $\Delta E = 0.180$ eV excitation function. These features are considered to be the outcome of resonance excitation, though each of them has its own origin and differs in major ways from the others. The nature and character of each of these resonant features will be discussed respectively in the following.

In the ground state, the methanol molecule has the electron configuration $\ldots(5a')^2(1a'')^2(6a')^2(7a')^2(2a'')^2(8a'\sigma^*)^0(9a'\sigma^*)^0(10a')^0(3a'')^0$, $^1A'$, or $\ldots(3sa')^0(3pa')^0(3pa')^0(3pa'')^0$ in the united atom, where the two lowest unfilled valence-shell molecular orbitals (MO's) of $(8a'\sigma^*)^0$ and $(9a'\sigma^*)^0$ are nearly identical to the $(3sa')^0$ and $(3pa')^0$ Rydberg orbitals of methanol [22–24]. It should be pointed out that the lowest unoccupied MO $8a'$, while being of the Rydberg type for small internuclear distances, will turn into an antibonding MO of σ^*(O-H) for larger internuclear separations [24]. Therefore, we may either use the description $3sa'$ when we would like to stress the relation to the higher members of the Rydberg series, or adopt the description $8a'\sigma^*$ when we want to determine the bonding properties of the MO's and/or the valence-shell character of the resulting electronic states. In fact, the first broad band centered at 6.7 eV in the far-UV absorption and energy-loss spectra of methanol has been assigned to either Rydberg excitation of $2a''\rightarrow 3sa'$ [25–27] or a $2a''\rightarrow 8a'\sigma^*$ valence transition [28–30], although the consensus seems to be that the band arises from both types of excitations (Rydberg-valence conjugates). Since it is the latter type that is of most interest in the present study, we shall take the view of the valence-shell MO description for the low-energy region of electronic excitation.

C. The TNI state(s) below 6 eV

The plateaulike feature between 3 and 6 eV is more notable in the ν_{12} excitation function in Fig. 3(b), which is related to the O-H bond of the molecule. Since the valence-shell MO $8a'\sigma^*$(OH) is, especially upon condensation, the only unoccupied orbital in this energy region available for the trapping of the incident electron, we are inclined to assign the feature in question to a valence-shell shape resonance of the electronic configuration written as $^2[N,(8a'\sigma^*)^1]$, $^2A'$, where N denotes the ground state $^1A'$ of methanol.

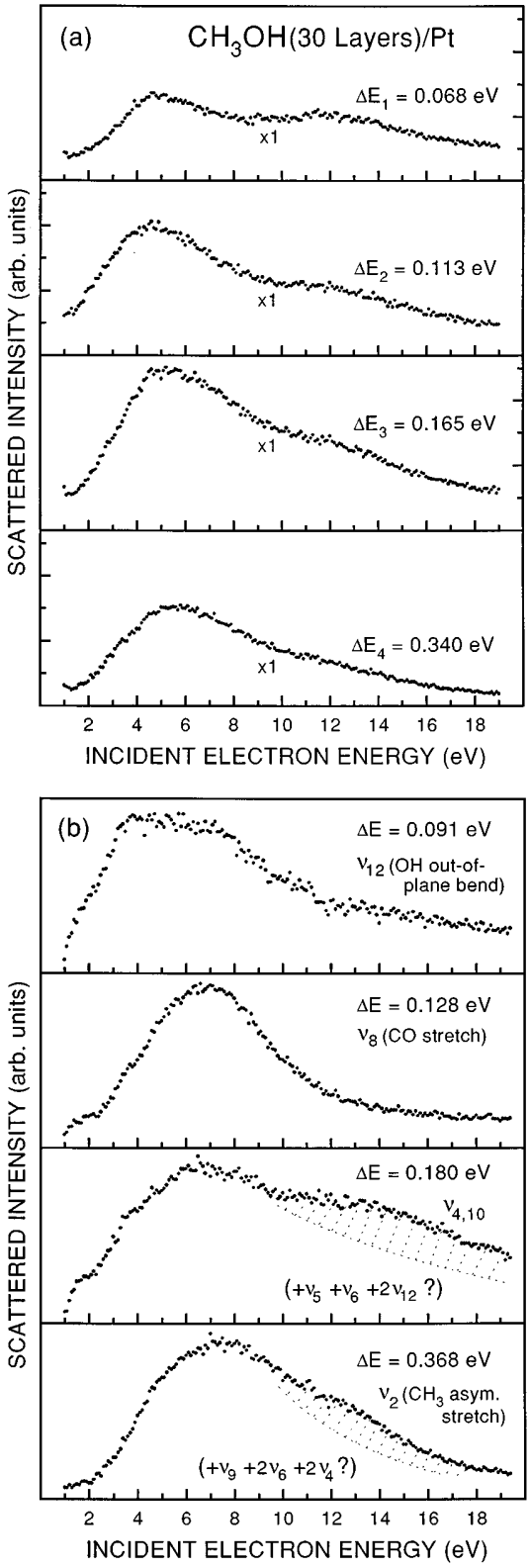

FIG. 3. (a) Energy dependences recorded for four background losses (ΔE) 68, 113, 165, and 340 meV in the energy range 1–20 eV. (b) Difference excitation functions obtained by subtracting the four energy-dependent curves of the background losses in (a), respectively, from the four raw excitation functions of the vibrational modes ν_{12}, ν_8, ν_4, and ν_2 in Fig. 2. The shaded area suggests the presence of a broadbandlike feature consisting of overlapping Feshbach resonances.

Although the resonance may have its center around 4.0 eV, its width cannot possibly be evaluated, since it eventually overlaps the next resonant structure. However, this shape resonance may decay via two totally different open channels: (a) one returns to the ground state $^1A'$ by the ejection of the extra electron (autodetachment), and (b) the other dissociates into stable neutral and negatively charged fragments (DEA). The width of the resonance is then closely related to these two partial widths. The resulting CH_3OH^- negative ions are very likely to undergo autodetachment, since this type of resonance is generally coupled strongly to its parent state. Apparently, no fine structure appears in the excitation functions, implying that the resonant state may be either repulsive, or relatively short lived such that very little vibration of the nuclei occurs during the lifetime of the resonance (the impulse limit [31]). On the other hand, however, some of the CH_3OH^- ions formed may have a sizeable survival probability [32] and therefore may reach the crossing point of the CH_3OH^- and CH_3OH potential-energy curves, at which CH_3OH^- is stabilized against the decay channel of autodetachment and starts to dissociate into $H+CH_3O^-$. This latter decay path is apparently supported by the DEA work on vapor-phase methanol [11], where the most intense signal of CH_3O^- has been found at 6.0 eV. It is of interest to note here that both the relatively broad line width perceived and the detection of CH_3O^- are suggestive of a repulsive potential-curve section in the Frank-Condon region, which is somehow consistent with the antibonding character of the $8a'\sigma^*$(OH) MO [32]. This could probably explain *in part* why this valence-shape resonance is more pronounced in the OH-mode-related excitation functions. Therefore, the broad resonant feature observed between 3 and 6 eV may represent a shape resonance occurring in the $8a'\sigma^*$ MO of the O-H valence bond. Going below this shape resonance, there appears a very weak, but perceivable bumplike feature between 1 and 2 eV in some of the excitation functions in Fig. 3(b). Presently, we have no adequate explanation for this feature.

D. The TNI structure between 6 and 10 eV

The structure in this region is best manifested in the 128-meV excitation function of Fig. 3(b). Centered around 7.0 eV, it has an apparently broad FWHM of almost 6 eV. However, the large width of the structure is not an unambiguous indication of the lifetime, since it may be governed by the Franck-Condon width of a dissociative state, or be due to several overlapping components. Indeed, both of the latter considerations are applicable here, and we consider that there may exist at least two, or perhaps three, TNI states beneath the bell-shaped structure; some of them, though different in origin, decay into H^- and CH_3O and/or CH_2OH.

The first of such resonant components, determined at the feature maximum around 7.0 eV, is attributed tentatively to a Feshbach-type resonance $^2A''$, with the Rydberg electronic configuration of $^2[(2a'')^1,(3sa')^2]$. The parent states of this resonance are both the singlet and triplet Rydberg states $^{3,1}[(2a'')^1,(3sa')^1]$ ($^{3,1}A''$), which, appearing at 6.7 eV in the vapor phase, has upshifted to 7.7 eV in the solid film [14] because of the condensed-phase effect [26,27]. The CH_3OH^- formed is considered to be dissociative, owing to the mixed antibonding character of the $3sa'$ orbital [22,23], and may undergo dissociation of the O-H bond, based on the experimental findings from the photodissociation study of the parent singlet state [33] as well as from the electron-impact dissociative attachment work of Parenteau, Jay-Gerin, and Sanche [13]. The latter work shows a shoulder feature at 7.3 eV appearing in the H^- total-yield spectrum of electron-stimulated desorption, which may be related to our 7.0-eV resonant feature.

The second resonant component in the region involves the methanol's second virtual valence MO $9a'\sigma^*$, which has a Rydberg conjugate orbital $3pa'$ (or $3p\sigma_1$, corresponding to $3pb_2$ in water [23]). Although theoretical studies of electron scattering by methanol are still scarce, calculations on water [34–36] have shown repeatedly a strong configuration mixing associated with the second unfilled valence $2b_2\sigma^*$ manifold and the Rydberg $3pb_2$ manifold. The very essence of such a computing outcome is expected to be applicable to methanol by virtue of the water's strong parentage. If correct, then methanol should also possess the $^{3,1}[(2a'')^1,(3pa')^1]$ and $^{3,1}[(2a'')^1,(9a'\sigma^*)^1]$ configurations that are Rydberg-valence conjugates [27]. The excited electronic states in question have, using electron impact, been observed for vapor-phase methanol around 7.7–7.8 eV [26,37] and their corresponding daughter TNI states—the Feshbach resonance $^2[(2a'')^1,(3pa')^2]$ and shape resonance $^2[N,(9a'\sigma^*)^1]$—are expected to be around this energy in the vapor phase, with the Feshbach state lying slightly below it. However, the $^2[(2a'')^1,(3pa')^2]$ Feshbach resonance is expected to be annihilated completely or blue-shift substantially upon condensation, because its electronic configuration involves strong Rydberg parentage [27]. On the other hand, except for some opposite energy shifts of the polarization and hydrogen bonding effects [6,14], the $^2[N,(9a'\sigma^*)^1]$ shape resonance $^2A'$ should remain essentially intact upon the same perturbation, since it is much less sensitive to condensed-phase effects. Therefore, the second resonant constituent of concern here should be the shape resonance $^2A'$, and it is most likely to lie near 7.5 eV. If assigned correctly, this shape resonance would correlate well with the 7.88-eV TNI resonant state determined for the vapor-phase methanol by electron-transmission spectroscopy (ETS) [10], and be in agreement also with Robin's [27] assignment of the $^2[N,(2b_2\sigma^*)^1]$ shape resonance to the water's 7.96-eV TNI resonant state [10]. Interestingly, the ETS 7.88-eV TNI state in vapor-phase methanol was considered by Robin [27] to bear a different origin than that of the water's 7.96-eV resonance. And it has since been assigned to a Feshbach-type resonance $^2A''$ of $^2[(2a'')^1,(3pa'')^2]$ instead, which has the $^{3,1}[(2a'')^1,(3pa'')^1]$ Rydberg states (about 8.32 eV [26] or 8.41 eV [23,27]) as its parents. This assignment was based chiefly on the standard Feshbach decrement of 0.50 eV with respect to the parent state. However, we believe that this $^2A''$ Feshbach resonance, if not totally obliterated, would be located somewhere around 9 eV in solid methanol due to the high-density ''pressure shift'' in the energy levels.

Given the fact that the second shape resonance $2A'$ involves an electron occupying the $9a'\sigma^*$ antibonding MO associated with the C-O valence bond, no one would be surprised at the sharp contrast of the line shape between the 128-meV excitation function, which describes essentially

the energy-dependent behavior of the C-O stretching mode ν_8 in methanol, and the others in Fig. 3(b). The idea of determining a meaningful width for this shape resonance may not, however, be practical due to the plausible involvement of other TNI states in the region. Yet the width of the ETS 7.88-eV resonant state was estimated to be fairly large (i.e., 3.8 eV FWHM) [10]. This value, along with the absence of fine structure in both phases, suggests that the resonance may be probed mostly within the repulsive part of the potential-energy curve and possess a relatively short lifetime. This is further supported by the gas-phase measurement on the OH^- anion yield of DEA [11], where the OH^- signal around 8 eV is notably small compared to the major peak at 10.5 eV, reflecting that most of the resonant TNI may have already autodetached even before reaching the crossing point of the potential-energy curves for the resonant state $^2A'$ and the ground state $^1A'$, or other low-lying electronic states. Although the second shape resonance is most likely to decay back to the ground state, with the release of the captured incident electron, a conclusion cannot be complete without theoretical calculations of the resonant energy-level system of CH_3OH^-.

The effect of resonance electron scattering is also evident in the 180- and 368-meV excitation functions, both of which are associated chiefly with the CH_3 asymmetric bending and stretching modes. A similar phenomenon has also been seen in the excitation functions of vapor-phase ethane (CH_3CH_3) [38] and methylamine (CH_3NH_2) [39], where a valence-shape resonance has been located at 7.5 eV and been considered as a consequence of trapping the electron in the σ^* MO of the C-C and C-N valence bonds, respectively. This correlates quite well with our second shape resonance occurring in the σ^*(C-O) MO. Thus, it appears that the resonant effect found in the mainly CH_3-related excitation functions may result largely from a major perturbation of the C-O valence bond owing to the occurrence of the second shape resonance. The unselective behavior of resonant vibrational excitation in the energy range 6–10 eV shown by all the excitation functions, however, may be regarded as the result of overlapping resonances taking place among the valence σ^* MO and Rydberg orbitals of the O-H and C-O bonds, which perturb the entire molecule.

There appears also some scattering intensity lying around 9 eV [more discernible in the 180- and 368-meV excitation functions of Fig. 3(b)]. This might have something to do with the Feshbach resonance $^2A'$ of $^2[(7a')^1,(3sa')^2]$, and perhaps also the $^2[(2a'')^1,(3pa'')^2]$ resonance $^2A''$, having the parent states of $^{3,1}[(7a')^1,(3sa')^1]$ and $^{3,1}[(2a'')^1,(3pa'')^1]$, respectively. The former, which appears at 8 eV in the vapor phase [12], has been observed near 9 eV, as the most intense feature, in the DEA H^- anion-yield spectrum of amorphous methanol [13]. Such a large H^- intensity may signify that the $^2A'$ Feshbach state is a reasonably longer-lived species and its contribution to the intensity of our excitation functions may therefore be relatively small. The latter $^2A''$ resonance, as projected by Robin [27], may shift upward from the lower-energy region; however, the scattering intensity it generates is expected to be fairly weak, based on the fact that its parent state $^1[(2a'')^1,(3p)^1]$, which is strikingly intense and even vibrationally structured in the vapor-phase energy-loss spectra [25,40], is obliterated in the condensed phase [14].

E. The TNI states beyond 10 eV

Both the 180- and 368-meV excitation functions show some relative increase in scattering intensity above 10 eV, as suggested by the shaded areas in Fig. 3(b), which are absent in the 128-meV excitation function of the strong dipole-active mode. Several Feshbach-type resonances may be formed in this energy region. Though perhaps overlapping each other, the first of these resonances is, with the configuration of $^2[(6a')^1,(3sa')^2]$ ($^2A'$), expected to lie between 11 and 12 eV; it has been detected at 10.5 eV in the vapor phase [12] and estimated to be around 11.5 eV in the condensed phase [13]. It may then be followed by two other similar Feshbach resonances: $^2[(1a'')^1,(3sa')^2]$ ($^2A''$) and $^2[(5a')^1,(3sa')^2]$, whose parent Rydberg states give rise to two very intense bandlike features (11–14 eV), superimposed on the $2a''$ and $7a'$ ionization continua, in the electron-energy-loss spectrum of vapor methanol [26]. Note, however, that all the parents of these three resonances have the electron transition terminating at the $3sa'$ Rydberg orbital of mixed O-H antibonding character, and thus might undergo dissociation of the O-H bond. It has been found that if the parent state is dissociative, the line width of the related Feshbach resonance can be considerably broadened so as to become undiscernable [27]. Hence, these resonances are expected to produce relatively weak broadband features extending over several electron volts.

In addition to this $3sa'$ series of Feshbach resonances, another series with core excitation terminating at $3p$ Rydberg orbitals may also possibly be involved in this broad band, as suggested by the DEA data of vapor methanol [11]. There, the O^- and OH^- yield functions of vapor methanol exhibit a predominant peak at 10.5 eV. Such anion fragments strongly imply the breaking of the C-O valence bond and hence the possible involvement of the $3pa'$ Rydberg orbital, which also bears the C-O antibonding character [23]. Starting around 10 eV, this series may perhaps be led by the Feshbach resonance ($^2A'$) of $^2[(7a')^1,(3pa')^2]$, whose parent would then be the Rydberg state $^1[(7a')^1,(3pa')^1]$ lying at 9.44 eV [23,37] in the vapor phase. The following two TNI states in line may be those $^2[(6a')^1,(3pa')^2]$ ($^2A'$) and $^2[(1a'')^1,(3pa')^2]$ ($^2A''$) Feshbach resonances. The parent of the latter, $^1[(1a'')^1,(3pa')^1]$ ($^1A''$), has been located at 12.9 eV in the vapor phase [26]. Yet the $3pa'$ series, if ever present, should be much weaker than its counterpart of the $3sa'$ series, as its parents have much lower profiles in the energy-loss spectra [26,37,40]. All the Feshbach resonances of this sort, overlapping or not, as a whole, may form a weak broad band in the high-energy region of the excitation functions.

IV. SUMMARY

We have reported the measurements of vibrational HREEL spectra and excitation functions for solid methanol film grown on a polycrystalline platinum foil held at 15 K within the impact-energy range of 1–20 eV in the large off-specular direction. The vibrational HREEL spectra obtained show that vibrations of solid methanol in its ground state are

quite sensitive to the variation of incident electron energy and the intensity of the vibrational losses can be enhanced substantially by resonance electron scattering.

The excitation functions recorded for the intramolecular fundamental vibrational modes exhibit three compound resonant states, located below 6 eV, between 6 and 10 eV, and beyond 10 eV, respectively. The plateaulike feature below 6 eV is attributed tentatively to the valence-type shape resonance $^2A'$ of the $^2[N,(8a'\sigma^*)^1]$ electronic configuration. The second valence-shape resonance $^2A'$ of $^2[N,(9a'\sigma^*)^1]$ appears around 7.5–8.0 eV and is surrounded by the Feshbach resonances, such as $^2[(2a'')^1,(3sa')^2]$ ($^2A''$, about 7 eV) and $^2[(7a')^1,(3sa')^2]$ ($^2A'$, about 9 eV). The shape resonance near 7–8 eV has also been observed in several other methanol-like molecules and seems to be a common occurrence. Both of the shape resonances are considered to be short lived and decay largely to the ground state of the molecule via autodetachment.

The weak, broadbandlike feature above 10 eV is tentatively assigned to a group of overlapping Feshbach resonances led by the $^2[(6a')^1,(3sa')^2]$ anion state, with possible overlapping with another group of the $^2[(7a')^1,(3pa')^2]$ configuration. Most of the Feshbach resonances discussed here are essentially considered to be dissociative and involved in with the two Rydberg orbitals $3sa'$ and $3pa'$ having a strong antibonding character. Their decay processes are expected to result in the rupture of the O-H and C-O bonds, forming negative ions, such as H^-, OH^-, and O^-.

All of the resonances reported here exhibit no fine structure. While the first shape resonance is observed largely in the excitation functions of those vibrational modes involving the OH group, the second strong band structure between 6 and 10 eV appears, in a much less selective fashion, in all the excitation functions of the fundamental vibrational modes of methanol investigated. The behavior of the latter may be associated with an occurrence of electron-attachment dissociation involving both the O-H and C-O bonds of methanol within the compound resonant states. Further theoretical work on the CH_3OH^- states and similar experimental studies in the vapor phase would be helpful in determining more precisely the nature of electron resonances in methanol.

ACKNOWLEDGMENTS

This work was supported by Le Conseil de Recherches Médicales du Canada. We are grateful to Marie-Josée Fraser for her assistance with the experimental work, and to Luc Parenteau for several useful discussions concerning his own work on methanol. One of us (A.T.W.) wishes to express his gratitude to Dr. Michael A. Hüels for the information on dissociative electron attachment that he has shared so generously, and for several illuminating confabulations, which were all fertile and valuable.

[1] L. Sanche, in *Excess Electrons in Dielectric Media*, edited by C. Ferradini and J. P. Jay-Gerin (CRC P, Boca Raton, FL, 1991), Chap. 1, p. 1; R. E. Palmer and P. J. Rous, Rev. Mod. Phys. **64**, 383 (1992).
[2] L. L. Kesmodel, Phys. Rev. Lett. **53**, 1001 (1984).
[3] T. S. Jones and N. V. Richardson, Phys. Rev. Lett. **61**, 1752 (1988).
[4] J. E. Demuth, D. Schmeisser, and Ph. Avouris, Phys. Rev. Lett. **47**, 1166 (1981).
[5] L. Sanche and M. Michaud, Phys. Rev. Lett. **47**, 1008 (1981).
[6] L. Sanche and M. Michaud, Phys. Rev. B **30**, 6078 (1984).
[7] M. Michaud and L. Sanche, Phys. Rev. A **36**, 4684 (1987).
[8] J. E. Turner, H. G. Paretzke, R. N. Hamm, H. A. Wight, and R. H. Ritchie, Radiat. Res. **92**, 47 (1982).
[9] L. G. Christophorou, in *Photon, Electron and Ion Probes of Polymer Structure and Properties*, ACS Symposium Series Vol. 162, edited by D. W. Dwight, T. J. Fabish, and H. R. Thomas (American Chemical Society, Washington, D.C., 1981), p. 11.
[10] D. Mathur and J. B. Hasted, Chem. Phys. Lett. **34**, 90 (1975).
[11] A. Kühn, H. P. Fenzlaff, and E. Illenberg, J. Chem. Phys. **88**, 7453 (1988).
[12] M. G. Curtis and I. C. Walker, J. Chem. Soc. Faraday. Trans. **88**, 2805 (1992).
[13] L. Parenteau, J. P. Jay-Gerin, and L. Sanche, J. Phys. Chem. **98**, 10 277 (1994).
[14] M. Michaud, M. J. Fraser, and L. Sanche, J. Chim. Phys. **91**, 1223 (1994).
[15] M. Michaud and L. Sanche, Phys. Rev. B **30**, 6067 (1984).
[16] M. Michaud and L. Sanche, Phys. Rev. A **36**, 4672 (1987).
[17] A. T. Wen, M. Michaud, and L. Sanche (unpublished).
[18] M. Falk and E. Whalley, J. Chem. Phys. **34**, 1554 (1961).
[19] G. Seng and F. Linder, Phys. B **9**, 2539 (1976); Y. Itikuwa, J. Phys. Soc. Jpn. **36**, 1127 (1974); N. Lane, in *Electron-Molecule Scattering*, edited by S. C. Brown (Wiley, New York, 1979), p. 147.
[20] J. W. Gadzuk, in *Vibrational Spectroscopy of Molecular Structure*, edited by J. T. Yates and T. E. Madey (Plenum, New York, 1987), p. 49.
[21] C. H. Li, S. Y. Tong, and D. L. Mills, Phys. Rev. B **21**, 3057 (1980).
[22] W. L. Jorgensen and L. Salem, *The Organic Chemist's Book of Orbitals* (Academic, New York, 1973).
[23] W. R. Wadt and W. A. Goddard III, Chem. Phys. **18**, 1 (1976).
[24] G. Herzberg, *Electronic Spectra of Polyatomic Molecules* (Van Nostrand Reinhold, New York, 1966).
[25] M. B. Robin and N. A. Kuebler, J. Electron Spectrosc. **1**, 13 (1972).
[26] M. B. Robin, *Higher Excited States of Polyatomic Molecules* (Academic, New York, 1974), Vol. I.
[27] M. B. Robin, *Higher Excited States of Polyatomic Molecules* (Ref. [26]), Vol. III.
[28] D. R. Salahub and C. Sandorfy, Chem. Phys. Lett. **8**, 71 (1971).
[29] D. N. Kirk, W. P. Mose, and P. M. Scopes, Chem. Commun. **81**, (1972).

[30] J. Texter and E. S. Stevens, J. Chem. Phys. **70**, 1440 (1979).
[31] G. J. Schulz, in *Principles of Laser Plasmas*, edited by G. Bekefi (Wiley, New York, 1976), p. 33.
[32] E. Illenberger and J. Momigny, *Gaseous Molecular Ions: An Introduction to Elementary Processes Induced by Ionization* (Springer, New York, 1992).
[33] S. Satyapal, J. Park, and R. Bersohn, J. Chem. Phys. **91**, 6873 (1989).
[34] W. A. Goddard III and W. J. Hunt, Chem. Phys. Lett. **24**, 464 (1974).
[35] M. Jungen, J. Vogt, and V. Staemmler, Chem. Phys. **37**, 49 (1979).
[36] G. H. F. Diercksen, W. D. Kraemer, T. N. Rescigno, C. F. Bender, B. V. McKoy, S. L. Langhoff, and P. W. Langhoff, J. Chem. Phys. **76**, 1043 (1982).
[37] W. C. Tam and C. E. Brion, J. Electron Spectrosc. **3**, 263 (1974).
[38] L. Boesten, H. Tanaka, M. Kubo, H. Sato, M. Kimura, M. A. Dillon, and D. Spence, J. Phys. B **23**, 1905 (1990).
[39] F. Motte-Tollet, M. J. Hubin-Franskin, and J. E. Collin, J. Chem. Phys. **93**, 7843 (1990).
[40] T. Yoshidome, H. Kawazumi, and T. Ogawa, J. Electron Spectrosc. **53**, 185 (1990).